  Bull. Chem. Soc. Jpn., 64, 1497—1508 (1991)

On the Facilitation Effect of Neutral Macrocyclic Ligands on the Ion Transfer across the Interface between Aqueous and Organic Solutions. I. Theoretical Equation of Ion-Transfer-Polarographic Current-Potential Curves and Its Experimental Verification

Hiroaki MATSUDA,* Yutaka YAMADA, Kazuo KANAMORI, Yoshihiro KUDO, and Yasuyuki TAKEDA

Department of Chemistry, Faculty of Science, Chiba University, Yayoi-cho 1-33, Chiba 260

(Received November 29, 1990)

A theoretical equation of the reversible polarographic current-potential curves for the ion transfer across the aqueous/organic interface facilitated by the neutral macrocyclic ligand present in the o-phase is derived without any limitation on the magnitude of distribution constant of the ligand. In two limiting cases, which have been employed in common experimental practice, i.e., (A) the bulk concentration of cation, c^*_M, in the aqueous phase $\gg$ that of ligand, c^*_L, in the organic phase and (B) the reverse condition, $c^*_M \ll c^*_L$, the equation of current-potential curves becomes the same in form as that of reversible D. C. polarographic waves. It is shown that the limiting current is controlled by diffusion of ligand in the organic phase for (A) and of cation in the aqueous phase for (B) and, on the other hand, the half-wave potential depends on c^*_M for (A) and on c^*_L for (B). Furthermore, an analysis method to determine the complex formation constants in the organic phase (and in the aqueous phase for favorable cases) from the concentration dependence of the half-wave potential is presented. The theoretical predictions are verified experimentally using dibenzo-18-crown-6 and 18-crown-6 as macrocyclic ligands and sodium, cesium, barium, and oxonium ions as transferred cations.

Natural and synthetic macrocyclic compounds, such as valinomysin, nonactin, and various crown ethers, are known to form selectively stable complexes with a variety of cations, especially alkali and alkaline-earth metal ions, by holding a cation in their central cavity, and then to allow the cation to be transferred from the aqueous phase (w-phase) into the organic phase (o-phase), because of the hydrophobic outer envelope of the complexes thus produced. This function of macrocyclic ligands has stimulated a great deal of interest in various branches of chemistry and biology. Potential applications have been made in liquid membrane ion-selective electrode and in making specific separations by solvent extraction and membrane transport methods. Liquid membrane containing macrocyclic compounds have also been recognized as a good model of the selective and up-hill ion transport through biological membranes.

In recent years, electrochemical methods have been employed for studies on the ion transfer across the water/nitrobenzene or water/1,2-dichloroethane interface facilitated by various natural and synthetic macrocyclic ligands. The studies done with electrochemical methods have been thoroughly reviewed by Koryta.[1-3] However, all the macrocyclic ligands hitherto employed have had large values of the distribution constant. Hence, it has been assumed that the ligands added to the o-phase cannot penetrate the w/o-interface and thus does not exist in the w-phase. Highly lipophilic crown ethers such as dibenzo-18-crown-6 (DB18C6) and its substituted derivatives have been used very frequently as the neutral carriers in ion-selective electrodes and in membrane transport experiments. On the other hand, unsubstituted crown ethers such as 15-crown-5 and 18-crown-6 (18C6), of which the distribution constants are relatively small, have been used for elucidating the behavior of crown ether complexes in the w-phase.

In the present paper, taking into account the above circumstances, we shall derive a theoretical equation of current–potential curves for the ion transfer across the w/o-interface facilitated by neutral macrocyclic ligands, without any limitation on the magnitude of distribution constant of the ligands. Then, the theoretical predictions obtained will be verified experimentally, using the ion-transfer-polarographic method with the electrolyte dropping electrode.[1]

Theory

In deriving a general equation of current-potential curves expressing the facilitation effect of neutral macrocyclic ligands on the ion transfer across the interface of the water drop growing into the organic solution, we shall make the following assumptions:

(i) The expanding plane model, which has been used as a good mathematical model for the dropping mercury electrode in polarography, is employed here for the moving interface between the water drop (w-phase) and the organic solution (o-phase). Then, the w/o-interface is taken as the origin of coordinates ($x=0$) and the w- and o-phases are placed in the regions: $-\infty \leqslant x \leqslant 0$ and $0 \leqslant x \leqslant +\infty$, respectively.

(ii) The complete dissociation of electrolytes present both in the w- and the o-phase is assumed for the sake of simplicity. Any effect of ion pair formation can be neglected.

(iii) At the beginning of the drop growth, the w-phase contains only the relevant metal ion M^{z+} at the uniform concentration c_M^*, except for indifferent electrolytes to be added if necessary, while the o-phase con-

tains the neutral macrocyclic ligand L at the uniform concentration c_L^* and an indifferent electrolyte.

(iv) Only the 1:1 complex ML^{z+} is formed in both phases. The rates of the complex formation and dissociation processes are sufficiently large in comparison with the corresponding diffusion rates, so that it may be assumed that the complex formation and dissociation are at equilibrium even when current is flowing. Then we have

$$\beta_1^\alpha = c_{ML}^\alpha / c_M^\alpha c_L^\alpha \quad (\alpha = w, o) \tag{1}$$

where c_j^α and β_1^α denote the concentration of the species j (j=M, L, ML) and the over-all formation constant of ML^{z+} in the α-phase, respectively.

An extention to the more general case, in which a series of complexes, such as 1:1, 1:2,$\cdots$, 1:n complexes, are formed under the presence of a large excess of the ligand in the o-phase, will be treated in a later section.

(v) The rates of transfer of all relevant species across the w/o-interface are sufficiently large in comparison with the corresponding diffusion rates,[4] so that the interfacial concentrations of all species in question satisfy the equilibrium relations, even when current is flowing. For the electrostatically neutral species L, we have

$$K_D = (c_L^o)_{x=0} / (c_L^w)_{x=0} \tag{2}$$

K_D denotes the distribution constant of L, which is assumed to be independent of the potential difference $\Delta\phi = \phi^w - \phi^o$ at the w/o-interface, where ϕ^α is the inner potential of the α-phase. On the other hand, the distribution constants of the charged species M^{z+} and ML^{z+} may depend on the potential difference and their potential dependence is assumed to be governed by the Nernst equation. Thus we have

$$\exp(\zeta'_M) = (c_M^o)_{x=0} / (c_M^w)_{x=0} \tag{3}$$

$$\exp(\zeta'_{ML}) = (c_{ML}^o)_{x=0} / (c_{ML}^w)_{x=0} \tag{4}$$

with

$$\zeta'_M = (zF/RT)(\Delta\phi - \Delta\phi^{o\prime}_M) \tag{5}$$

$$\zeta'_{ML} = (zF/RT)(\Delta\phi - \Delta\phi^{o\prime}_{ML}) \tag{6}$$

where $\Delta\phi_j^{o\prime}$ is termed the formal potential of the species j for the ion transfer across the w/o-interface. Frequently, the following stoichiometric equation is employed for the facilitated ion trasfer across the w/o-interface:

$$M^{z+}(\text{w-phase}) + L(\text{o-phase}) \rightleftharpoons ML^{z+}(\text{o-phase}) \tag{7}$$

For this process the Nernst equation may be written as

$$\exp(\zeta'_{M/ML}) = (c_{ML}^o)_{x=0} / (c_M^w)_{x=0} (c_L^o)_{x=0} \tag{8}$$

with

$$\zeta'_{M/ML} = (zF/RT)(\Delta\phi - \Delta\phi^{o\prime}_{M/ML}), \tag{9}$$

where $\Delta\phi^{o\prime}_{M/ML}$ denotes the formal potential of the process expressed by Eq. 7. Taking into consideration the relations expressed by Eqs. 1—6, we can readily verify that the following relations hold among $\Delta\phi^{o\prime}_M$, $\Delta\phi^{o\prime}_{ML}$ and $\Delta\phi^{o\prime}_{M/ML}$:

$$\Delta\phi^{o\prime}_{ML} = \Delta\phi^{o\prime}_M - (RT/zF)\ln(K_D\beta_1^o/\beta_1^w) \tag{10}$$

$$\begin{aligned}\Delta\phi^{o\prime}_{M/ML} &= \Delta\phi^{o\prime}_M - (RT/zF)\ln\beta_1^o \\ &= \Delta\phi^{o\prime}_{ML} - (RT/zF)\ln(K_D/\beta_1^w)\end{aligned} \tag{11}$$

(vi) For simplicity we assume that the diffusion coefficients of relevant species in the α-phase (α=w, o) have the common value D^α.

(vii) Any interfacial excess of the relevant species, due to adsorption etc., is assumed to be absent at the w/o-interface.

Under the assumptions (i)—(vii) described above, the boundary value problem for the diffusion processes of the species M^{z+}, L and ML^{z+} can be formulated, as follows:

$$\mathscr{D}^\alpha c_M^\alpha = R_1^\alpha \tag{12}$$

$$\mathscr{D}^\alpha c_L^\alpha = R_1^\alpha \tag{13}$$

$$\mathscr{D}^\alpha c_{ML}^\alpha = -R_1^\alpha \quad (\alpha = w, o) \tag{14}$$

with

$$R_1^\alpha = k_1^\alpha (c_{ML}^\alpha - \beta_1^\alpha c_M^\alpha c_L^\alpha) \tag{15}$$

where the diffusion operator for the expanding plane model, $\mathscr{D}^\alpha$, defined by

$$\mathscr{D}^\alpha = \partial/\partial t - D^\alpha \partial^2/\partial x^2 - (2x/3t)\partial/\partial x, \tag{16}$$

is employed for simplicity of description and k_1 denotes the rate constant of the dissociation process of ML^{z+}. The initial and boundary conditions are derived from the assumptions (iii), (vi), and (vii), as follows:

$$t = 0 : \left\{ \begin{array}{lll} c_M^w = c_M^*, & c_L^w = 0, & c_{ML}^w = 0 \\ c_M^o = 0, & c_L^o = c_L^*, & c_{ML}^o = 0 \end{array} \right\} \tag{17}$$

$$\left. \begin{array}{l} x \to -\infty : c_M^w = c_M^*, \quad c_L^w = 0, \quad c_{ML}^w = 0 \\ x \to +\infty : c_M^o = 0, \quad c_L^o = c_L^*, \quad c_{ML}^o = 0 \end{array} \right\} \tag{18}$$

$$x = 0 : \begin{cases} (f_M)_t = -\{D^w(\partial c_M{}^w/\partial x) + D^w(\partial c_{ML}{}^w/\partial x)\} \\ \quad = D^o(\partial c_M{}^o/\partial x) + D^o(\partial c_{ML}{}^o/\partial x) \quad (19) \\ (f_L)_t = -\{D^w(\partial c_L{}^w/\partial x) + D^w(\partial c_{ML}{}^w/\partial x)\} \\ \quad = D^o(\partial c_L{}^o/\partial x) + D^o(\partial c_{ML}{}^o/\partial x) \quad (20) \end{cases}$$

where $(f_j)_t$ denotes the total flux of the species j (j=M, L) at the w/o-interface. Here, it is noticed that in spite of the assumption (iv) the reaction term R_1 must be added to the diffusion equations of individual species. The reasoning is: since the equilibrium condition given by Eq. 1 is approached only when k_1^α approaches infinity, the term R_1^α becomes indeterminate. This difficulty can be avoided by introducing the total concentrations of the metal ion and the ligand, defined by

$$(c_M^\alpha)_t = c_M^\alpha + c_{ML}^\alpha \quad (21)$$

$$(c_L^\alpha)_t = c_L^\alpha + c_{ML}^\alpha \quad (\alpha = w, o) \quad (22)$$

Then, our diffusion problem can be reduced to

$$\mathscr{D}^\alpha(c_M^\alpha)_t = 0 \quad (23)$$

$$\mathscr{D}^\alpha(c_L^\alpha)_t = 0 \quad (24)$$

with the initial and boundary conditions:

$$\left.\begin{matrix} t = 0 \\ x \to \pm\infty \end{matrix}\right\} : \left\{\begin{matrix} (c_M{}^w)_t = c_M{}^*, \ (c_L{}^w)_t = 0 \\ (c_M{}^o)_t = 0, \quad (c_L{}^o)_t = c_L{}^* \end{matrix}\right\} \quad (25)$$

$$x = 0 : \begin{cases} (f_M)_t = -D^w\{\partial(c_M{}^w)_t/\partial x\} = D^o\{\partial(c_M{}^o)_t/\partial x\} & (26) \\ (f_L)_t = -D^w\{\partial(c_L)_t/\partial x\} = D^o\{\partial(c_L{}^o)_t/\partial x\} & (27) \end{cases}$$

The boundary value problem expressed by Eqs. 23—27 has already been solved in a previous paper,[5] in which it has been shown that the following relations hold between the total interfacial concentration $\{(c_j^\alpha)_t\}_{x=0}$ and the corresponding flux $(f_j)_t$:

$$\{(c_M{}^w)_t\}_{x=0} = c_M{}^* - (D^w)^{-1/2} I_M \quad (28)$$

$$\{(c_M{}^o)_t\}_{x=0} = (D^o)^{-1/2} I_M \quad (29)$$

$$\{(c_L{}^w)_t\}_{x=0} = -(D^w)^{-1/2} I_L \quad (30)$$

$$\{(c_L{}^w)_t\}_{x=0} = c_L{}^* + (D^o)^{-1/2} I_L \quad (31)$$

with

$$I_j = \left(\frac{7}{3\pi}\right)^{1/2} \int_0^t \frac{(f_j)_t u^{2/3} du}{(t^{7/3} - u^{7/3})^{1/2}} \quad (j = M, L) \quad (32)$$

Hence we obtain immediately from Eqs. 28—31

$$\{(c_M{}^w)_t\}_{x=0} + \xi\{(c_M{}^o)_t\}_{x=0} = c_M{}^* \quad (33)$$

$$\{(c_L{}^w)_t\}_{x=0} + \xi\{(c_L{}^o)_t\}_{x=0} = \xi c_L{}^* \quad (34)$$

where

$$\xi = (D^o/D^w)^{1/2} \quad (35)$$

Substituting the relations expressed by Eqs. 1—4 and 10 into Eqs. 33 and 34 and performing some calculations yields

$$(c_M{}^w)_{x=0}\{(1 + \exp\zeta_M) + \beta_1{}^w(1 + \exp\zeta_{ML})(c_M{}^w)_{x=0}\} = c_M{}^* \quad (36)$$

$$(c_L{}^w)_{x=0}\{(1 + \xi K_D) + \beta_1{}^w(1 + \exp\zeta_{ML})(c_M{}^w)_{x=0}\} = \xi c_L{}^* \quad (37)$$

with

$$\zeta_M = \zeta'_M + \ln\xi = (zF/RT)(\Delta\phi - \Delta\phi_M^{o\prime}) + \ln(D^o/D^w)^{1/2} \quad (38)$$

$$\zeta_{ML} = \zeta'_{ML} + \ln\xi = (zF/RT)(\Delta\phi - \Delta\phi_{ML}^{o\prime}) + \ln(D^o/D^w)^{1/2} \quad (39)$$

Eliminating $(c_M{}^w)_{x=0}$ from Eqs. 36 and 37, we obtain the algebraic equation of the second order with respect to $(c_L{}^w)_{x=0}$, the solution of which is

$$(c_L{}^w)_{x=0} = \xi c_L{}^*(1 - \Psi)/(1 + \xi K_D) \quad (40)$$

with

$$\Psi = \frac{2\gamma_M}{\left[\left(1 + \frac{1 + \xi K_D}{\beta_1^w c^*}\,\frac{1 + \exp\zeta_M}{1 + \exp\zeta_{ML}}\right) + \left\{\left(1 + \frac{1 + \xi K_D}{\beta_1^w c^*}\,\frac{1 + \exp\zeta_M}{1 + \exp\zeta_{ML}}\right)^2 - 4\gamma_M\gamma_L\right\}^{1/2}\right]} \quad (41)$$

$$c^* = c_M{}^* + \xi c_L{}^* \quad (42)$$

$$\gamma_M = c_M{}^*/c^*, \quad \gamma_L = \xi c_L{}^*/c^* \quad (\gamma_M + \gamma_L = 1) \quad (43)$$

Substituting Eq. 40 into Eq. 36 and performing some rearrengements yields

$$(c_M{}^w)_{x=0} = (c_M{}^* - \xi c_L{}^*\Psi)/(1 + \exp\zeta_M) \quad (44)$$

Introducing Eqs. 40 and 44 into Eq. 1 with α=w, we obtain

$$(c_{ML}{}^w)_{x=0} = \xi c_M{}^*\Psi/(1 + \exp\zeta_{ML}) \quad (45)$$

The current flowing, i, is defined as the total amount

of the net positive charges transferred from the w- to the o-phase per unit time. Hence, the current can be related to the total flux of metal ion at the interface, $(f_M)_t$, as follows:

$$i = zFA(t)(f_M)_t \tag{46}$$

where $A(t)$ denotes the surface area of the water drop. If the water drop is assumed to be a complete sphere as for the dropping mercury electrode in polarography, we obtain

$$A(t) = 4\pi(3vt/4\pi)^{2/3} \tag{47}$$

where v is the constant volume flow rate of aqueous solution.

Therefore, substituting Eqs. 44—46 into Eq. 28 yields

$$\left(\frac{7}{3\pi}\right)^{1/2}\int_0^t \frac{(i/zFA)u^{2/3}\mathrm{d}u}{(t^{7/3}-u^{7/3})^{1/2}} = \frac{\sqrt{D^w}\,c_M^*}{1+\exp(-\zeta_M)} + \left\{1 - \frac{1+\exp(-\zeta_{ML})}{1+\exp(-\zeta_M)}\right\}\frac{\sqrt{D^o}\,c_L^*\Psi}{1+\exp(-\zeta_{ML})} \tag{48}$$

This is the Abel integral equation with respect to (i/zFA), which can readily be solved by using the standard method.[6] Thus we obtain

$$i = i_M + \left\{1 - \frac{1+\exp(-\zeta_{ML})}{1+\exp(-\zeta_M)}\right\} i_{fw} \tag{49}$$

where

$$i_M = (i_d)_M/[1+\exp(-\zeta_M)] \tag{50}$$

$$i_{fw} = (i_d)_L\Psi/[1+\exp(-\zeta_{ML})] \tag{51}$$

with

$$(i_d)_M = \sqrt{7/3\pi}\; zFA(t)\sqrt{D^w}\,c_M^*/\sqrt{t} \tag{52}$$

$$(i_d)_L = \sqrt{7/3\pi}\; zFA(t)\sqrt{D^o}\,c_L^*/\sqrt{t} \tag{53}$$

Here, $(i_d)_M$ and $(i_d)_L$ denote the limiting diffusion currents, expressed by the Ilkovic equation, which are obtained when the currents would be controlled completely by the diffusion processes of M in the w-phase and of L in the o-phase, respectively. Equation 49 with Eqs. 50 and 51 is the general expression for the reversible current–potential curves. The first term on rhs of Eq. 49 denotes the current due to the transfer of M^{z+}, which would be obtained without adding L to the o-phase, while the second term expresses the current facilitated by the presence of L in the o-phase.

Now, our consideration will be resticted to the case, in which well-defined facilitated waves are observed at sufficiently more negative potentials than $\Delta\phi_M^{o\prime}$. Then, within the potential region where the facilitated wave appears, we have

$$\exp(-\zeta_M) \longrightarrow \infty$$

Hence the facilitated current is given by i_{fw}, the expression of which can be given, after introducing the explicit expression for Ψ, as follows:

$$i_{fw} = \frac{(i_d)_M + (i_d)_L}{1+\exp(-\zeta)} \times \frac{2\gamma_M\gamma_L}{1+\left\{1 - 4\gamma_M\gamma_L\left(\frac{1+\exp(-\zeta_{ML})}{1+\exp(-\zeta)}\right)^2\right\}^{1/2}} \tag{54}$$

where

$$\left.\begin{aligned}\gamma_M &= \frac{c_M^*}{c^*} = \frac{(i_d)_M}{(i_d)_M + (i_d)_L},\\ \gamma_L &= \frac{c_L^*}{c^*} = \frac{(i_d)_L}{(i_d)_M + (i_d)_L}\end{aligned}\right\} \tag{43'}$$

$$\begin{aligned}\zeta &= \zeta_{ML} - \ln\{(1+\xi K_D + \beta_1^w c^*)/\beta_1^w c^*\}\\ &= \zeta_M - \ln\{(1+\xi K_D + \beta_1^w c^*)/K_D\beta_1^o c^*\}\end{aligned} \tag{55}$$

Under the limiting current conditions we have

$$\exp(-\zeta) \longrightarrow 0 \text{ and } \exp(-\zeta_{ML}) \longrightarrow 0$$

Hence, the limiting current, $(i_{fw})_{lim}$, can be given as

$$(i_{fw})_{lim} = \begin{cases} (i_d)_L \text{ for } c_M^* > \xi c_L^* \ (\gamma_L/\gamma_M < 1) & (56)\\ (i_d)_M \text{ for } \xi c_L^* > c_M^* \ (\gamma_M/\gamma_L < 1) & (56') \end{cases}$$

This equation indicates that the limiting current is controlled only by the diffusion process of the species with smaller bulk concentration.

If we solve Eq. 54 with respect to $\Delta\phi$, the formula of current-potential curves can be rewritten as

$$\begin{aligned}\Delta\phi = \Delta\phi_M^{o\prime} &- \frac{RT}{zF}\ln\xi\\ &+ \frac{RT}{zF}\ln\left\{\frac{1+\xi K_D + \beta_1^w c^*[1-2\gamma_M\gamma_L(x_M+x_L)]}{K_D\beta_1^o c^*(1-x_M)(1-x_L)/(x_M+x_L)}\right\}\\ &+ \frac{RT}{zF}\ln\frac{1}{2}\left\{1+\left[1-4\gamma_M\gamma_L(1-x_M)(1-x_L)\right.\right.\\ &\left.\left.\times\left(\frac{\beta_1^w c^*}{1+\xi K_D+\beta_1^w c^*[1-2\gamma_M\gamma_L(x_M+x_L)]}\right)^2\right]^{1/2}\right\}\end{aligned} \tag{57}$$

with

$$x_M = i_{fw}/(i_d)_M, \quad x_L = i_{fw}/(i_d)_L \tag{58}$$

The half-wave potential can be obtained by introducing into Eq. 57 $i_{fw}=\frac{1}{2}(i_d)_L$ for $c_M^* \geqslant \xi c_L^*$ and $i_{fw}=\frac{1}{2}(i_d)_M$ for $\xi c_L^* \geqslant c_M^*$, respectively, as follows:

$$\Delta\phi_{1/2} = \begin{cases} \Delta\phi_M^{o\prime} - \dfrac{RT}{zF}\ln\xi + \dfrac{RT}{zF}\left[\ln\left(\dfrac{1+\xi K_D+\beta_1^w c_M^*}{K_D\beta_1^o c_M^*}\right)\right. \\ -\ln\left(1-\dfrac{1}{2}\dfrac{\gamma_L}{\gamma_M}\right) \\ +\ln\dfrac{1}{2}\left\{1+\left[1-\left(\dfrac{\gamma_L}{\gamma_M}\right)\left(2-\dfrac{\gamma_L}{\gamma_M}\right)\right.\right. \\ \left.\left.\left.\times\left(\dfrac{\beta_1^w c_M^*}{1+\xi K_D+\beta_1^w c_M^*}\right)^2\right]^{1/2}\right\}\right] \\ \qquad \text{for } c_M^* \geqslant \xi c_L^* \ (\gamma_L/\gamma_M \leqslant 1) \qquad (59) \\ \Delta\phi_M^{o\prime} - \dfrac{RT}{zF}\ln\xi + \dfrac{RT}{zF} \\ \text{[terms obtained by exchanging } c_M^* \text{ and } \xi c_L^*\text{]} \\ \qquad \text{for } \xi c_L^* > c_M^* \ (\gamma_M/\gamma_L < 1) \qquad (59') \end{cases}$$

In most experimental practice, the two limiting conditions, i.e., (A) $c_M^* \gg \xi c_L^*$ and and (B) $\xi c_L^* \gg c_M^*$, have been employed, in order to simplify analysis of current-potential curves. In the following we shall examine these two cases in some detail.

(A) $c_M^* \gg c_L^*$

When the condition:

$$\gamma_L/\gamma_M = \xi c_L^*/c_M^* \leqslant \frac{z}{25}\left(1+\frac{\beta_1^w c_M^*}{1+\xi K_D}\right) \tag{60}$$

is satisfied, the general formula of facilitated waves can be simplified very much within errors of ca. 1 mV and Eq. 57 can be reduced to

$$\Delta\phi = \Delta\phi_{1/2}^A + (RT/zF)\ln[i_{fw}/\{(i_d)_L - i_{fw}\}] \tag{61}$$

with

$$\Delta\phi_{1/2}^A = \Delta\phi_M^{o\prime} - \frac{RT}{zF}\ln\xi + \frac{RT}{zF}\ln\left(\frac{1+\xi K_D+\beta_1^w c_M^*}{K_D\beta_1^o c_M^*}\right) \tag{62}$$

Hence the log-plots of the current-potential curve, i.e., $\log[i_{fw}/\{(i_d)_L - i_{fw}\}]$ vs. $\Delta\phi$ plots, yield a straight line with a reciprocal slope of 2.3 (RT/zF), as in D. C. polarography. Equation 62 indicates that the half-wave potential depends only on the bulk concentration of metal ion, which is present in the w-phase in a large excess in comparison with the bulk concentration of ligand in the o-phase. Figure 1 is a schematic diagram showing the concentration dependence of the half-wave potential. As can readily be seen from the figure, the behavior of the concentration dependence can be divided into three types, as follows:

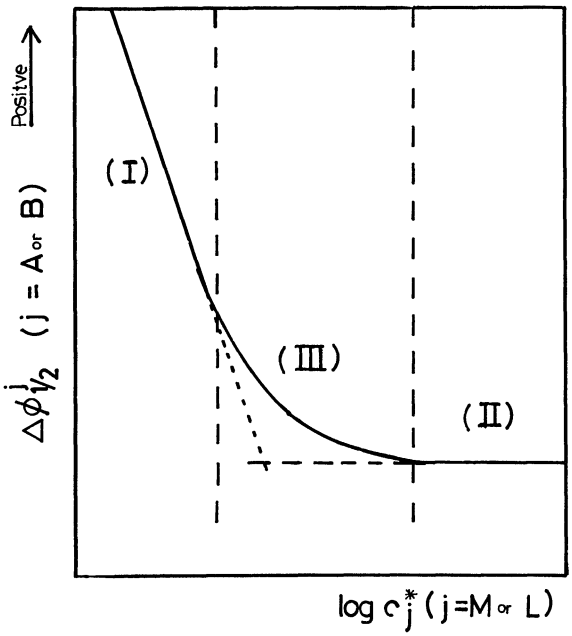

Fig. 1. Schematic diagram showing the concentration dependence of the half-wave potential. $\Delta\phi_{1/2}^A$ vs. $\log c^*_M$ plot for the cell (A). $\Delta\phi_{1/2}^B$ vs. $\log c^*_L$ plot for the cell (B).

Type (I): The plots of $\Delta\phi_{1/2}^A$ vs. $\log c_M^*$ yields a straight line with the slope of -2.3 (RT/zF). This type can be obtained when the following condition is satisfied:

$$(1+\xi K_D) \geqslant 20\ \beta_1^w c_M^* \tag{63}$$

Type (II): The half-wave potential becomes independent of $\log c_M^*$ and the plot of $\Delta\phi_{1/2}^A$ vs $\log c_M^*$ gives a horizontal line. For this type the following inequality holds:

$$\beta_1^w c_M^* \geqslant 20(1+\xi K_D) \tag{64}$$

Type (III): This is the intermediate type between the types (I) and (II). In this case we have

$$(1+\xi K_D) \sim \beta_1^w c_M^* \tag{65}$$

In order to analyze the concentration dependence of the half-wave potentials precisely, we introduce the following function F_A:

$$F_A \equiv \exp(zF/RT)(\Delta\phi_{1/2}^A - \Delta\phi_M^{o\prime})$$
$$= (\beta_1^w/\xi K_D\beta_1^o) + \{(1+\xi K_D)/\xi K_D\beta_1^o\}(1/c^*_M) \tag{66}$$

Then the plots of the function F_A vs. $(1/c_M^*)$ yields a straight line, of which the slope and the intercept are $\{(1+\xi K_D)/\xi K_D\beta^o{}_1\}$ and $(\beta^w{}_1/\xi K_D\beta^o{}_1)$, respectively. Hence, if the value of ξK_D is known, we can determine the values of the complex formation constants both in the w- and the o-phase from the slope and the intercept, respectively. In practice, however, it frequently happens that the $\Delta\phi^A_{1/2}$ vs. $\log c_M^*$ curve belongs to the type (I) and the F_A vs. $(1/c_M^*)$ plot passes through the origin within experimental errors. In such a case we can obtain only the value of the complex formation constant in the o-phase from the slope. For the complex formation constant in the w-phase we obtain only the following inequality condition from Eq. 63:

$$\beta_1^w \leqslant (1 + \xi K_D)/\{20(c_M^*)_{max}\} \tag{67}$$

where $(c_M^*)_{max}$ denotes the maximum concentration of metal ion employed in the experiment. On the other hand, in some case the concentration dependence of the half-wave potential belongs to the type (II) and the F_A vs. $(1/c_M^*)$ plot becomes a horizontal line within experimental errors. In this case only the ratio $(\beta^w{}_1/\beta^o{}_1)$ is determinable from the intercept, and from Eq. 64 we have the following inequality condition:

$$\beta_1^w \geqslant 20(1 + \xi K_D)/(c_M^*)_{min} \tag{68}$$

where $(c_M^*)_{min}$ is the minimum concentration of metal ion used in the experiment.

(B) $c_L^* \gg c_M^*$

For the case:

$$\gamma_M/\gamma_L = c_M^*/\xi c_L^* \leqslant \frac{z}{25}\left(1 + \frac{\xi\beta_1^w c_L^*}{1 + \xi K_D}\right) \tag{69}$$

the general equation 57 can be simplified to

$$\Delta\phi = \Delta\phi^B_{1/2} + (RT/zF)\ln[i_{fw}/\{(i_d)_M - i_{fw}\}] \tag{70}$$

with

$$\Delta\phi^B_{1/2} = \Delta\phi^{o\prime}_M - \frac{RT}{zF}\ln\xi + \frac{RT}{zF}\ln\left(\frac{1 + \xi K_D + \xi\beta_1^w c_L^*}{\xi K_D\beta_1^o c_L^*}\right) \tag{71}$$

within errors of ca. 1 mV. Further we introduce the following function F_B:

$$F_B \equiv \exp(zF/RT)(\Delta\phi^B_{1/2} - \Delta\phi^{o\prime}_M) = (\beta_1^w/\xi K_D\beta_1^o) + \{(1 + \xi K_D)/\xi K_D\beta_1^o\}(1/\xi c^*{}_L) \tag{72}$$

Equations 70—72 can also be obtained by exchanging c_M^* by ξc_L^* in Eqs. 61, 62, and 66, respectively. Hence, all arguments described above in (A) may be applicable to the present case.

Extention to More General Case. It has been known in solvent extraction and membrane transport experiments that when the ionic crystal diameter of metal ion is somewhat larger than the cavity size of macrocyclic ligands, the 1:2 complex, i.e., the so-called sandwich type complex, as well as the ordinary 1:1 complex are formed under the presence of a large excess of the macrocyclic ligands in the o-phase. Hence, we shall extend the above theory to the more general case, in which a series of complex species ML_p^{z+} (p=1, 2,$\cdots$, n) are formed under the condition (B).

In this case, the total concentrations of the metal ion and the ligand are defined as

$$(c_M^\alpha)_t = c_M^\alpha + \sum_{p=1}^{n} c_{ML_p}^\alpha \tag{73}$$

$$(c_L^\alpha)_t = c_L^\alpha + \sum_{p=1}^{n} p c_{ML_p}^\alpha \quad (\alpha = w,\ o) \tag{74}$$

Then these two total concentrations satisfy the diffusion boundary value problem defined by Eqs. 23—27 and thus the solutions are given by Eqs. 28—31. The successive complex formation in the α-phase may be characterized by the following over-all formation constant:

$$\beta_p^\alpha = c_{ML_p}^\alpha/c_M^\alpha(c_L^\alpha)^p \quad (\alpha = w,\ o;\quad p = 1,\ 2,\cdots,\ n) \tag{75}$$

On the other hand, the transfer of complex species ML_p^{z+} (p=0, 1, 2, $\cdots$, n) across the w/o-interface may be governed by the Nernst equation:

$$\exp(\zeta'_{ML_p}) = (c_{ML_p}{}^o)_{x=0}/(c_{ML_p}{}^w)_{x=0} \tag{76}$$

with

$$\zeta'_{ML_p} = (zF/RT)(\Delta\phi - \Delta\phi^{o\prime}_{ML_p}) \tag{77}$$

where $\Delta\phi^{o\prime}_{ML_p}$ is the formal potential of the complex species ML_p^{z+} for the ion transfer across the w/o-interface and may be related to $\Delta\phi^{o\prime}_M$ as follows:

$$\Delta\phi^{o\prime}_{ML_p} = \Delta\phi^{o\prime}_M - (RT/zF)\ln(K_D^p\beta_p^o/\beta_p^w) \tag{78}$$

Hence, introducing Eqs. 75 and 76 into Eqs. 33 and 34 yields

$$(c_M{}^w)_{x=0}\{(1 + \exp\zeta_M) + \sum_{p=1}^{n}\beta_p{}^w(1 + \exp\zeta_{ML_p})[(c_L{}^w)_{x=0}]^p\} = c_M^* \tag{79}$$

$$(c_L{}^w)_{x=0}\{(1 + \xi K_D) + (c_M{}^w)_{x=0}\sum_{p=1}^{n} p\beta_p{}^w(1 + \exp\zeta_{ML_p})[(c_L{}^w)_{x=0}]^p\} = \xi c_L^* \tag{80}$$

Elimination of $(c_M{}^w)_{x=0}$ from the above two equations

results in an algebraic equation of $(n+1)$-th order with respect to $(c_L^w)_{x=0}$. Under the condition (B), in which $c_L^* \gg c_M^*$ holds, this $(n+1)$-th order algebraic equation can be factorized and the solution becomes

$$(c_L^w)_{x=0} = \xi c_L^*/(1 + \xi K_D) \quad (81)$$

Hence, we can obtain the expression for $(c_M^w)_{x=0}$ by substituting Eq. 81 into Eq. 79 and then the expression of $(c_{ML_p}^w)_{x=0}$ can be derived from introducing $(c_M^w)_{x=0}$ thus obtained and Eq. 81 into Eq. 75. Substituting the interfacial concentrations of a series of complex species obtained in this way into Eq. 73 and performing some calculation by using the Eq. 78, we have

$$\{(c_M^w)_t\}_{x=0} = c_M^*/\{1 + \exp(zF/RT)(\Delta\phi - \Delta\phi_{1/2}^B)\} \quad (82)$$

with

$$\Delta\phi_{1/2}^B = \Delta\phi_M^{\circ\prime} - \frac{RT}{zF}\ln\xi + \frac{RT}{zF}\ln\left\{\frac{1 + \sum_{p=1}^{n}\beta_p^w[\xi c_L^*/(1 + \xi K_D)]^p}{1 + \sum_{p=1}^{n}\beta_p^\circ[\xi K_D c_L^*/(1 + \xi K_D)]^p}\right\} \quad (83)$$

Hence, introducing Eqs. 46 and 82 into Eq. 28 yields the Abel integral equation similar to Eq. 48, the solution of which gives for current–potential curves

$$i = (i_d)_M/\{1 + \exp(zF/RT)(\Delta\phi - \Delta\phi_{1/2}^B)\} \quad (84)$$

where $\Delta\phi_{1/2}^B$ is the half-wave potential given by Eq. 83. Of course, for $n=1$ Eq. 83 can be reduced to Eq. 71.

Very frequently, especially for hydrophobic macrocyclic ligands, the following conditions are satisfied:

$$K_D \gg 1, \quad K_D \gg (\beta_p^w)^{1/p} c_L^*$$

In such a case Eq. 83 may be reduced to

$$\Delta\phi_{1/2}^B = \Delta\phi_M^{\circ\prime} - (RT/zF)\ln\xi - (RT/zF)\ln\{1 + \sum_{p=1}^{n}\beta_p^\circ(c_L^*)^p\} \quad (85)$$

This equation is the same in form as that of the reversible half-wave potential for the polarographic reduction of complex metal ions. Therefore, by using the DeFord–Hume method[7] in polarography, we can determined the values of β_p° $(p=1, 2, \cdots, n)$ succesively from the concentration dependence of the half-wave potential.

Experimental

Chemicals. Nitrobenzene, employed as the o-phase, was purified by the method described by Kakutani et al.[4] Four-times distilled water was used to prepare the aqueous electrolyte solutions. Tetrabutylammonium tetraphenylborate (TBATPB), which was used as the supporting electrolyte in the o-phase, was prepared by the equimolar addition of an aqueous solution of sodium tetraphenylborate (Kanto Chemical Co.) to an aqueous solution of tetrabutylammonium chloride (Kanto Chemical Co.). The resulting precipitate was solved into 1,2-dichloroethane (DCE), washed repeatedly with distilled water, and then recrystallized by pouring the DCE solution into distilled ethanol. Commercial DB18C6 (Merck, Schuchardt) and 18C6 (Nippon Soda Co.) were recrystallized from benzene and acetonitrile, and dried under reduced pressure. All other chemicals were of analytical grade and used without further purification. The nitrobenzene solution of TBATPB and the aqueous solution were equilibrated with each other by shaking overnight before use.

Electrochemical Measurements. The electrolysis cell employed here is essentially the same as that described by Kihara and Yoshida,[8] except for wearing the water jacket around the cell. The cell temperature was controlled at 25±0.3 °C by circulating thermostated water through the jacket. The aqueous solution was dropped upword into the nitrobenzene solution from a teflon capillary (diameter 0.8 mm) with the volume flow rate $v=(5—15)\times10^{-3}$ cm^3 s^{-1} and the drop time $t_d=2—5$ s. The potential difference at the test electrode was controlled by means of a four-electrode potentiostat (Husoseisakusho, defferential potentiostat HECS 310B) with a positive feedback circuit for iR compensation.

The galvanic cells employed for the control or the measurement of the potential difference at the w/o-interface were the following two cells, corresponding to the conditions (A) $(c^*_M \gg c^*_L)$ and (B) $(c^*_L \gg c^*_M)$, respectively:

Cell (A):

(RE1) Ag	AgCl	0.05 mol dm^{-3} TBACl	0.05 mol dm^{-3} TBATPB + y mmol dm^{-3} L	*	z mol dm^{-3} M^{I}Cl or M^{II}Cl$_2$	sat. KCl salt bridge	0.05 mol dm^{-3} NaCl	AgCl	Ag (RE2)
		I (w)	II (o)		III (w)		IV (w)		

Cell (B):

(RE1) Ag	AgCl	0.05 mol dm^{-3} TBACl	0.05 mol dm^{-3} TBATPB + y' mol dm^{-3} L
		I (w)	II (o)

z' mmol dm^{-3} M^{1}Cl + 0.1 mol dm^{-3} $MgSO_4$	sat. KCl salt bridge	0.05 mol dm^{-3} NaCl
III (w)		IV (w)

AgCl | Ag (RE2)

Here the test interface is marked by asterisk and L and M denote the macrocyclic ligand and the cation in question, respectively. The reference electrode for the nitrobenzene phase, RE1, was a Ag|AgCl|0.05 mol dm^{-3} TBACl(W) electrode, which was connected to nitrobenzene phase II through sintered glass. On the other hand, the reference electrode for the aqueous phase, RE2, was a Ag|AgCl|0.05 mol dm^{-3} NaCl(W) electrode and connected to aqueous phase III through a salt-bridge containing saturated KCl solution. For the cell (B), 0.1 mol dm^{-3} $MgSO_4$ was added to the aqueous phase III as a supporting electrolyte. Two counter electrodes were platinum wires immersed in two aqueous MCl solutions, which, in turn, were connected to the aqueous phase I and III through sintered glass, respectively. The linear sweep voltage was applied at the rate of 2 mV s^{-1} by means of a potential scanner (Huso seisakusho, potential sweep unit HECS 321B) and polarograms were recorded using a X-Y recorder (Graphtec Co., WX 1200).

The voltage, V_{app}, applied to the cells was defined as the potential of the terminal of RE2, E_{RE2}, against to that of RE1, E_{RE1}, i.e., $V_{app}=E_{RE2}-E_{RE1}$. Therefore, if we neglect the potential difference through the salt bridge, we obtain $V_{app}=\Delta\phi$ +const. The constant term was evaluated under the well-known extrathermodynamic assumption that the standard transfer free energies of tetraphenylarsonium cation ($TPhAs^+$) and tetraphenylborate anion ($TPhB^-$) are equal,[9] as follows: using the cells (A) and (B) in the absence of any ligand in the o-phase, we measured the half-wave potential of tetramethylammonium ion (TMA^+), from which we determined the formal potential, $(\Delta\phi^{o'}_{TMA})_{meas}$, after correcting the diffusion coefficient term $(RT/F)\ln\sqrt{D^o/D^w}=-0.009$ V.[10] Since the literature value of $\Delta\phi^{o'}_{TMA}$ under the TPhAs-TPhB assumption is 0.035 V,[2] we have $\Delta\phi=V_{app}-[(\Delta\phi^{o'}_{TMA})_{meas}-0.035\ V]$. The values of potential $\Delta\phi$ given in the present paper are those calculated in this way and designated as V vs. TPh(As/B)E.

The flow of the positive charge from the w- to the o-phase was taken as the positive current. The current values used for the wave-form analysis were corrected appropriately for the residual currents which were obtained using the cells in the absence of ligands in the o-phase.

Results and Discussion

In the following we shall verify experimentally the theoretical predictions obtained above, especially for the two limiting conditions (A) and (B). As typical macrocyclic ligands we employ DB18C6 and 18C6, of which the distribution constants are very large (K_D=2.3×10^4)[11] and relatively small (K_D=0.10),[11] respectively. On the other hand, sodium, cesium, barium, and oxonium ions are chosen as the cations yielding facilitated waves. The wave-form analysis is performed in the same mannar as in the polarographic practice.

DB18C6.

(1) DB18C6-Na^+ System. First, we examine the behavior of DB18C6-Na^+ complex, using both the cells (A) and (B). The well-defined facilitated waves were always observed at the potentials 150—200 mV more negative than the final rise. The limiting currents were diffusion-controlled with respect to the ligand in the o-phase for the cell (A) and to the metal ions in the w-phase for the cell (B), as proved from the fact that the diffusion current constant, defined by

$$(I_d)_j = (i_d)_j/m^{2/3}t_d^{1/6}c^*_j \quad (j = L \text{ or } M),$$

was constant within experimental errors, when values of c^*_j (0.2—1 mmol dm^{-3}), v (5—15×10^{-3} cm^3 s^{-1}) and t_d (2—6 s) were changed. The ratio, $(I_d)_L/(I_d)_M$, of the diffusion current constants obtained for the cells (A) and (B), respectively, was 0.50. The log-plots of current-potential curves yielded straight lines with the reciprocal slopes of 61±2 mV/decade for the cell (A) and of 63±1 mV/decade for the cell (B). These facts indicate that the facilitated waves of DB18C6-Na^+ system are reversible and diffusion-controlled.

In Fig. 2, the half-wave potentials obtained both for the cells (A) and (B), $\Delta\phi^A_{1/2}$ and $\Delta\phi^B_{1/2}$, are given in

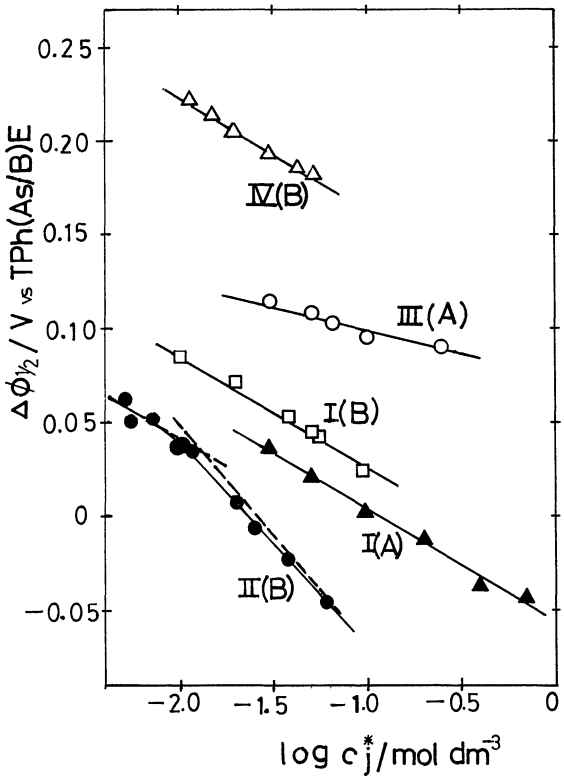

Fig. 2. Half-wave potentials of the DB18C6 complexes in dependence of log c^*_j (j=M for the cell (A) and L for the cell (B)). I: Na^+, II: Cs^+, III: Ba^{2+}, and IV: H_3O^+. (A) and (B) denote the kind of cell employed.

dependence of $\log c^*_M$ and $\log c^*_L$ by the curves I(A) and I(B), respectively. For both cases, we have straight lines with the slope of −60 mV/decade, indicating that the DB18C6–Na^+ system corresponds to the type (I) described in Fig. 1. As can readily be seen from Fig. 2, the straight line I(A) is located at ca. 20 mV more negative potential than that of I(B). Comparing Eq. 62 with Eq. 71 yields for $c^*_M=c^*_L$

$$\Delta\phi^A_{1/2} - \Delta\phi^B_{1/2} = (RT/zF)\ln\xi \quad (86)$$

Therefore, this value of −20 mV may be comparable to the theoretical prediction of −18 mV, which can be calculated from the above equation with $\xi=(I_d)_L/(I_d)_M=0.50$.

In Fig. 3, the values of functions F_A and F_B calculated from Eqs. 66 and 72 with $\Delta\phi^\circ_{Na}=0.355$ V vs. TPh(As/B)E[12] are plotted against $(1/c^*_j)$ (j=M for I(A) and L for I(B)). These plots fall on straight lines with the slope of 1.3×10^{-7} mol^{-1} dm^3 for I(A) and 2.8×10^{-7} mol^{-1} dm^3 for I(B) and with the intercept of zero for both I(A) and I(B) within experimental errors. The fact that the slope of I(B) is ca. 2.1 times larger than that of I(A) may be explained from the following relation: [slope of F_B vs. $(c^*_L)^{-1}$ plot]/[slope of F_A vs. $(c^*_M)^{-1}$ plot]$=\xi^{-1}$, which can be derived from Eqs. 66 and 72.

As described in the theoretical part, we can evaluate the complex formation constant in the o-phase from the value of slope to be $\log\beta^\circ_1=6.8$. On the other hand, the formation constant in the w-phase cannot be determined, sicne the value of intercept becomes zero. From Eq. 67 we obtain only the following inequality condition: $\log\beta^w_1<2.9$. In this connection the literature value of $\log\beta^w_1$ is 1.16.[13]

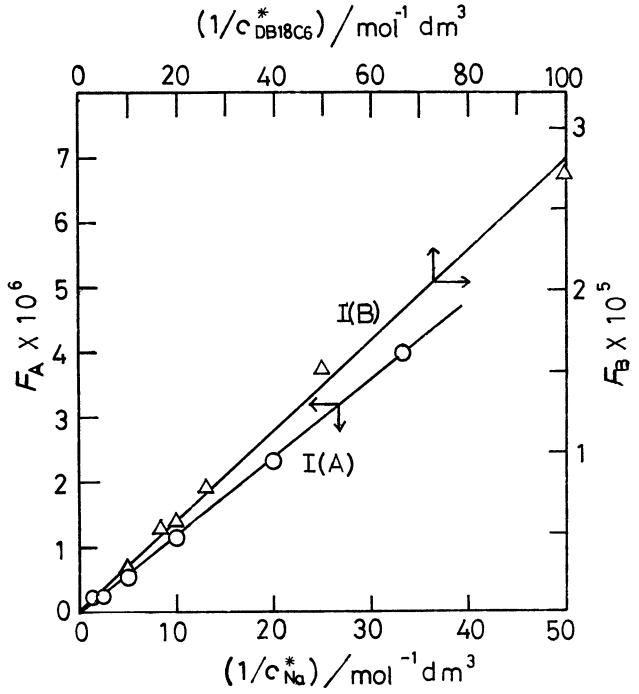

Fig. 3. F_A vs. $(1/c^*_{Na})$ and F_B vs. $(1/c^*_{DB18C6})$ plots for DB18C6–Na^+ system. I(A): F_A vs. $(1/c^*_{Na})$, I(B): F_B vs. $(1/c^*_{DB18C6})$.

(2) DB18C6–Cs^+ System. As is well-known, cesium ion is bulky compared with the other alkali metal ions, so that the standard ion-transfer potential becomes relatively negative. Hence, if we employ the cell (A), the corresponding potential window becomes very narrow, and we cannot observe any well-defined facilitated wave. On this ground, the behavior of facilitated waves of cesium ion was examined only for the cell (B).

In the absence of ligand in the o-phase, we observed a well-defined wave at the potential ca. 100 mV more negative than the final rise, which was regarded as being due to the transfer of cesium simple ion across the w/o-interface. This wave was reversible and diffusion-controlled, as verified from the constancy of diffusion current constant and the log-plot analysis of current–potential curves. The half-wave potential obtained is 0.131 V vs. TPh(As/B)E.

Addition of DB18C6 in the o-phase in a large excess (c_L^*=5—40 mmol dm^{-3}) shifted the wave of cesium ion to the potential region +0.06—−0.05 V vs. TPh(As/B)E. The limiting currents of these facilitated waves are diffusion-controlled with respect to Cs^+, as verified from the constancy of diffusion-current constant. The log-plots of current-potential curves yield straight lines with the reciprocal slope of 63±3 mV/decade. The half-wave potentials determined from log-plots are given in dependence of $\log c_L^*$ by curve II(B) in Fig. 2. As can readily be seen from figure, curve II(B) is asymptotic to a straight line with the slope of −120 mV/decade at high ligand concentration, while it approaches a straight line with the slope of −60 mV/decade with a decrease in ligand concentration. In accord with the fact that the ionic radius of Cs^+ (1.67 Å)[14] larger than the cavity radius of DB18C6 (1.34—1.43 Å),[15] this result suggests that the cesium ion forms the so-called sandwich type 1:2 (metal to ligand) complex with DB18C6 at higher ligand concentration. Since K_D-value of DB18C6 is very large (2.3×10^4) and the literature value of $\log\beta_1^w$ is 0.83,[13] the concentration dependence of the half-wave potential may be expressed by Eq. 85. Hence, we can evaluate the values of β°_p (p=1, 2, ···) by means of the DeFord–Hume method[7] in polarography. We define the DeFord–Hume F_o-function as

$$F_o \equiv \exp(zF/RT)\{(\Delta\phi^B_{1/2})_M - \Delta\phi^B_{1/2}\} = 1 + \sum_{p=1}^{n}\beta_p^\circ(c^*_L)^p \quad (87)$$

where $(\Delta\phi^B_{1/2})_M$ denotes the half-wave potential of simple cesium ion. Then, we define, in general, the DeFord–Hume F_p-function (p=1, 2, ···) as

$$F_p = \{F_{p-1} - \lim(c_L^* \longrightarrow 0)F_{p-1}\}/c_L^* \quad (88)$$

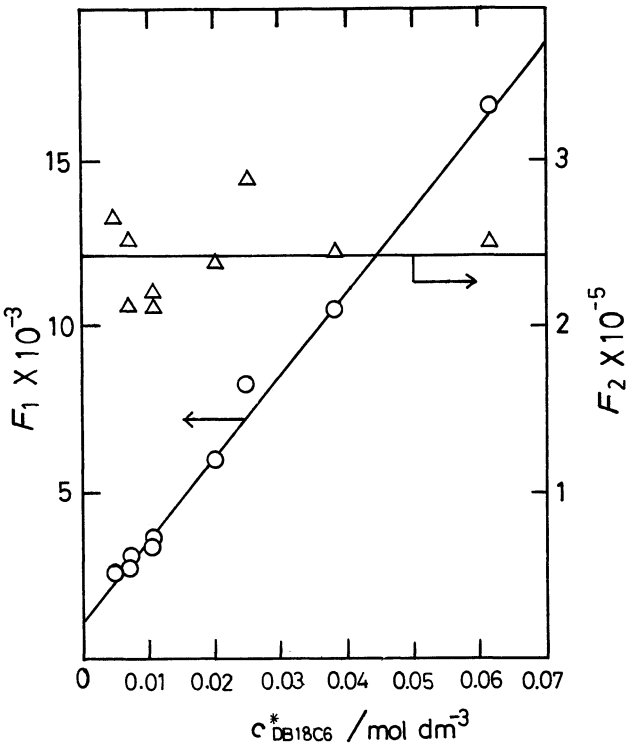

Fig. 4. DeFord-Hume functions F_1 and F_2 in dependence of c^*_L for the DB18C6-Cs^+ system.

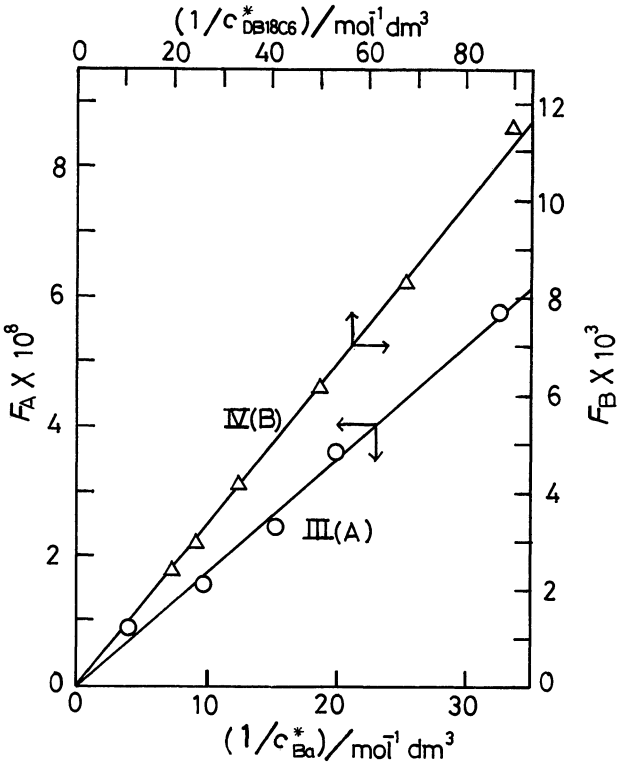

Fig. 5. F_A vs. $(1/c^*_{Ba})$ plot for the DB18C6-Ba^{2+} system and F_B vs. $(1/c^*_{DB18C6})$ plot for the DB18C6-H_3O^+ system. III(A): DB18C6-Ba^{2+}, IV(B): DB18C6-H_3O^+.

where $\lim(c_L^* \to 0)F_p$ denotes the value of F_p extrapolated to $c_L^*=0$, which is equal to β^o_p, as can be seen from Eqs. 87 and 88. In this way, from the extrapolated values of F_p (p=1, 2, ···) vs. c_L^* plots, we can evaluate succesively the values of β^o_1, β^o_2, ···.

In Fig. 4, the DeFord-Hume functions F_1 and F_2 are plotted against c_L^*, where the experimentally determined value of 0.131 V vs. TPh(As/B)E is employed for $(\Delta\phi^B_{1/2})_{Cs}$. As can be seen from the figure, the extrapolated values of these functions yield $\log \beta^o_1=3.1$ and $\log \beta^o_2=5.4$.

(3) DB18C6-Ba^{2+} System. As an example of alkaline earth metal ions, we examined the behavior of barium ion, using the cell (A). The well-defined facilitated waves were always observed at the potential ca. 100 mV more negative than the final rise. The limiting currents were verified to be diffusion-controlled with respect to the ligand and the value of diffusion current constant was ca. 1.8 times larger than that of DB18C6-Na^+ complex obtained for the cell (A). The log-plot analysis of current-potential curves yielded straight lines with the reciprocal slope of 32±2 mV/decade. These results indicate that these facilitated waves correspond to the reversible transfer of divalent cation across the w/o-interface as can readly be expected. The half-wave potentials determined from the log-plot analysis are plotted against the logarithm of Ba^{2+} bulk concentration in Fig. 2 (see curve III(A)). This plot yields a straight line with the slope of −28 mV/decade, indicating that the DB18C6-Ba^{2+} system corresponds to the type (I). The F_A vs. $(1/c^*_{Ba})$ plot is given by curve III(A) in Fig. 5, where the values of F_A have been calculated using the literature value $\Delta\phi^o_{Ba}=0.328$ V vs. TPh(As/B)E.[2] We can see that this plot yields a straight line passing through the origin within experimental errors. Since $K_D \gg 1$, we can obtain directly from the slope the value of $\log \beta^o_1$ as 8.8. For the value of β^w_1, from Eq. 64 we have only the inequality equation, $\log \beta^w_1 < 3.0$, while the literature value of $\log \beta^w_1$ is 1.95.[13]

(4) DB18C6-H_3O^+ System. The facilitation effects of DB18C6 on oxonium ion were small, so that we employed here only the cell (B), because we could not separate the facilitated waves from the final rise for the cell (A) containing a large excess of oxonium ion in the w-phase. The facilitated waves were observed at the potenitals only 40—60 mV more negative than the final rise. Hence the data obtained were rather inaccurate comparing with those of other cases, although corrections for residual currents were carried out as carefully as possible. The limiting currents were proved to be diffusion-controlled from the constancy of diffusion current constant. The log-plot analysis yielded straight lines with a reciprocal slope of 56±4 mV/decade, though the data were fairly scattered. The plot of half-wave potentials vs. $\log c_L^*$ yields a straight line with the

slope of −61 mV/decade, as shown by curve IV(B) in Fig. 2. The plot of F_B vs. $(1/c^*_L)$ is shown by curve IV(B) in Fig. 5, where F_B values have been calculated with $\Delta\phi^\circ_H$=0.337 V vs. TPh(As/B)E.[12] As can be seen from the figure, this plot yields a straight line passing through the origin. For the cell (B), we can obtain from the slope the value of log $(\xi\beta^o{}_1)$ as 3.7. The value of ξ for this complex was estimated as follows: the diffusion current constant $(I_d)_H$ is 1.5 times larger than that of Na^+ obtained for the cell (B). Further, the value of ξ for the DB18C6–Na^+ system is 0.5, as given above. Hence the value of ξ for DB18C6–H_3O^+ system may be estimated to be 0.5/1.5=0.33. Using this value of ξ yields log $\beta^o{}_1$=4.2.

18C6.

Since the K_D-value of 18C6 is 0.10, the interfacial concentration of L in the w-phase may become 10 times larger than that of the o-phase. Hence, the diffusion layer formed in the vicinity of the w/o-interface in the w-phase may be presumed to become unstable, especially for the cell (B) for which the ligand is present in a large excess. On this ground, we examined the behavior of current–potential curves only for the cell (A). Even when the cell (A) was employed, a gradual decrease in the limiting current was observed during repeating measurements for a long time, due to loss of ligand from the o- to the w-phase. Hence, in order to obtain reproducible results, it was required to start measurements as soon as possible after constructing the cell.

(1) 18C6-Na^+ System. The well-defined facilitated waves were obtained at the potentials about 160 mV more negative than the final rise, with the diffusion-controlled limiting currents with respect to the ligand concentration. The log-plot analysis of current–potential curves yielded straight lines with the reciprocal slope of 63±4 mV/decade. The half-wave potentials in dependence of log c^*_{Na} are shown by curve I(A) in Fig. 6. As can be seen from the behavior of the curve, the concentration dependence of the half-wave potential belongs to the intermediate type(III). The F_A vs. $(1/c^*_M)$ plot is given in Fig. 7, from which we can see that the plot points fall on a straight line with non-zero values of both the slope and the intercept. Hence, we can fortunately, in this case, determine the formation constants both in the w- and the o-phase. Using K_D=0.10 and assuming ξ=0.5 yields log $\beta^w{}_1$=0.7 and log $\beta^o{}_1$=8.5. The former value may compare with the literature value of log $\beta^w{}_1$=0.8 obtained by calorimetry.[16]

(2) 18C6-Ba^{2+} System. The 18C6–Ba^{2+} complex yields well-defined facilitated waves at the potentials 100 mV more negative than the final rise, with limiting currents controlled by diffusion of the ligand. The log-plot analysis of current–potential curves gives straight lines with the reciprocal slope of 32±3 mV/decade, indicating that the transfered ion is divalent. The concentration dependence of the half-wave potential is given by curve III(A) in Fig. 6, from which we can see that the

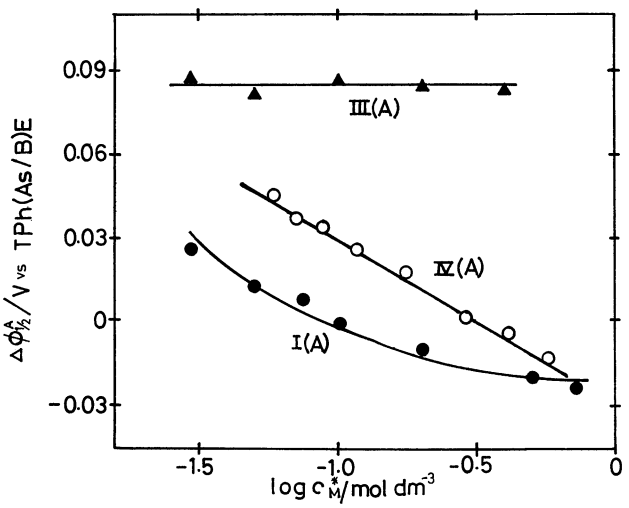

Fig. 6. Half-wave potentials of the 18C6 complexes in dependence of log c^*_M. I(A): Na^+, III(A): Ba^{2+}, and IV(A): H_3O^+.

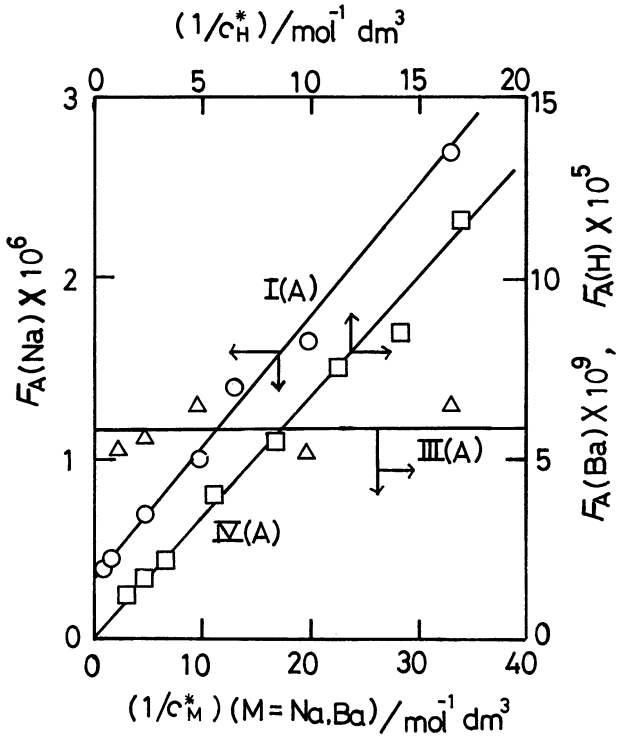

Fig. 7. F_A vs. $(1/c^*_M)$ plots for the 18C6–Na^+, –Ba^{2+}, and –H_3O^+ systems. I(A): 18C6-Na^+, III(A): 18C6–Ba^{2+}, IV(A): 18C6–H_3O^+.

half-wave potential is independent of the Ba^{2+}-concentration and this system belongs to the type (II). The F_A vs. $(1/c^*_{Ba})$ plot yields a straight line with zero slope within experimental errors, as seen from Fig. 7. Hence, we can obtain only the ratio $\beta^o{}_1/\beta^w{}_1$ from the value of intercept. Using K_D=0.10 and ξ=0.5 yields log $(\beta^o{}_1/\beta^w{}_1)$= 9.5. If we use the literature value of 3.87 for log $\beta^w{}_1$,

which has been obtained by Izatt et al.[16] using calorimetry, we obtain $\log \beta^{o}{}_{1}=13.4$. On the other hand, from Eq. 68 we obtain the following inequality equation: $\log \beta^{w}{}_{1}>3$, which is consistent with the literature value.

(3) 18C6-H_3O^+ System. Finally we examined the behavior of oxonium ion. In contrast to the DB18C6-H_3O^+ system, the 18C6-H_3O^+ system exhibited well-defined facilitated waves at the potential ca. 120 mV more negative than the final rise, with diffusion-controlled limiting currents with respect to the ligand concentration. The log-plot analysis of current-potenial curves yielded straight lines with the reciprocal slope of 59±3 mV/decade. The half-wave potentials obained are plotted against $\log c^{*}{}_{H}$ in Fig. 6 (curve IV(A)). As can be seen from the figure, this plot gives a straight line with the slope of −57 mV/decade, indicating that the 18C6-H_3O^+ system belongs to the type (I). In Fig. 7, the values of F_A are plotted against $(1/c_L^*)$, from which we can see that this plot yields a straight line passing through the origin, in spite of small K_D-value of 18C6. From the value of slope we obtain $\log \beta^{o}{}_{1}=7.5$, where ξ is assumd to be 0.5, since for the cell (A) the diffusing species in both the w- and o-phases may be regarded as the ligand. On the other hand, for $\beta^{w}{}_{1}$, we have only the inequality equation: $\log \beta^{w}{}_{1}\leqslant -1$, from Eq. 67. Hence it can be seen that the formation constant of oxonium ion in the w-phase is very small.

In conclcusion, it can be stated that the theoretical equation derived without any limitation on the magnitude of distribution constants of macrocyclic ligands explaines extensively the behavior of facilitated ion transfer across the water/introbenzene interface and allows to evaluate the complex formation constants in the nitrobenzene phase and for favorable cases those of both the nitrobenzene and water phase.

In the present paper we have selected the polarographic method with the electrolyte dropping electrode from various electrochemical methods available at present. However, the theoretical equations obtained here can easily be transformed to those of other various polarographic and voltammetric techniques in the same manner as done in usual polarography and voltammetry.

References

1) J. Koryta, *Electrochim. Acta,* **24**, 293 (1979).
2) J. Koryta, *Electrochim. Acta,* **29**, 445 (1984).
3) J. Koryta, *Electrochim. Acta,* **33**, 189 (1988).
4) T. Kakutani, Y. Nishiwaki, T. Osakai, and M. Senda, *Bull. Chem. Soc. Jpn.,* **59**, 781 (1986).
5) H. Matsuda and Y. Ayabe, *Bull. Chem. Soc. Jpn.,* **28**, 422 (1955); H. Matsuda, *Z. Elektrochem.,* **61**, 489 (1957).
6) K. Hidaka, "Oyo-sekibunhoteishiki-ron," (Applied theory of integral equations), Kawade-shobo, Tokyo (1943), pp. 130—134.
7) D. D. DeFord and D. N. Hume, *J. Am. Chem. Soc.,* **73**, 5321 (1951).
8) S. Kihara, M. Suzuki, K. Maeda, K. Ogura, S. Umetani, M. Matsui, and Z. Yoshida, *Anal. Chem.,* **58**, 2954 (1986).
9) A. J. Parker, *Electrochim. Acta,* **21**, 671 (1976).
10) T. Osakai, T. Kakutani, and M. Senda, *Bull. Chem. Soc. Jpn.,* **57**, 370 (1984).
11) T. Iwachido, M. Minami, A. Sadakane, and K. Toei, *Chem. Lett.,* **1977**, 1511.
12) J. Rais, *Collect. Czeck. Chem. Commun.,* **36**, 3253 (1971).
13) E. Shchori, N. Nae, and J. Jagur-Grodzinski, *J. Chem. Soc., Dalton Trans.,* **1975**, 2381.
14) R. D. Shannon and C. T. Prewitt, *Acta Crystallogr., Sect. B,* **25**, 925 (1969).
15) J. D. Lamb, R. M. Izatt, and J. J. Christensen, "Progress in Macrocyclic Chemistry," ed by R. M. Izatt and J. J. Christensen, J. Wiley & Sons, New York, N. Y. (1981), Vol. 2, Chap. 2, pp. 41—90.
16) R. M. Izatt, R. E. Terry, B. L. Haymore, L. D. Hansen, N. K. Dalley, A. G. Avondet, and J. J. Christensen, *J. Am. Chem. Soc.,* **98**, 7620 (1976).